6.4.2 Worn surfaces and subsurface of Al-Si-X sliding pins

A. Examination by XRD

Figure 6.17 presents the XRD spectra from the worn surface of the Al-25SiCuMg (PT) alloy after sliding under various loads. Before sliding, the surface was found to contain α-Al, Si and a little Al_2Cu (Fig. 6.17 a). After it had been worn at 27 N, the surface had constituents similar to those before wearing (Fig. 6.17 b). When the load increased to 87N, the worn surface had a notable quantity of α-Al_2O_3 oxide (Fig. 6.17 c), suggesting that a remarkable oxidation had occurred during sliding under such a high load. Figure 6.17 c did not reveal any Fe-Al or Fe-Al-O intermetallic phases on the worn surface, indicating that most of the iron that was transferred from disc surface may only be mechanically mixed with aluminum alloys or turned into nano-sized Fe-Al or Fe-Al-O compound particles. Finally, the oxide that had formed earlier on the worn surface disappeared after seizure (Fig. 6.17 d), revealing that the oxide layer was removed during sliding under seizure load.

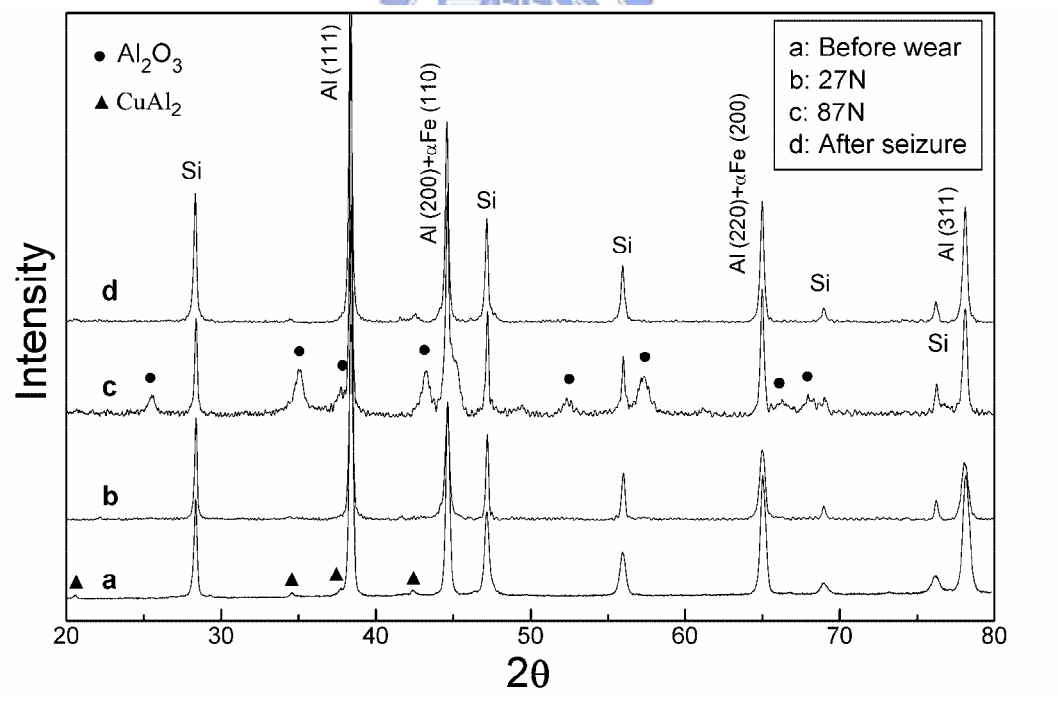

Figure 6.17 XRD on the worn surfaces of as-prepared Al-25SiCuMg (PT) (a) before wearing, and (b) after wearing at a load of 27N, (c) at a load of 87N, and (d) after seizure occurring.

The formation of oxide on worn surface under heavy load wearing was also observed for the Al-20SiFe (PT) alloy (Fig. 6.18). The Al-20SiFe before wearing is composed of α-Al, Si, and some β- Al_5SiFe together with a minorδ-Al_4FeSi_2 (Fig. 6.18 a). After wearing at 116N (in region III, referred to Fig. 6.12a), some additionalα-Al_2O_3 oxides appeared on the worn surface (Fig. 6.18 b). It is worthy to note that because α-Fe overlaps the peaks of α-Al, variation of Fe content can not be revealed only using these XRD spectra. The trace of Fe on the worn surfaces was found by SEM examination on the worn surfaces or wear debris, which were detailed in following paragraphs.

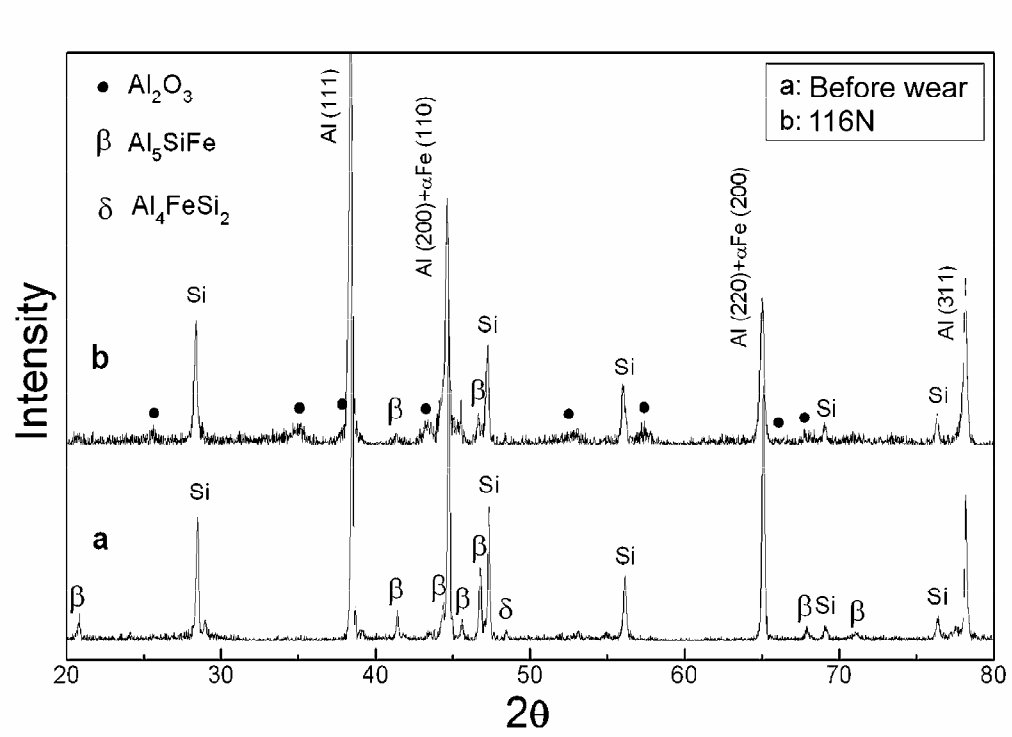

Figure 6.18 XRD analyses obtained on the worn surface of the Al-20Si-5Fe (PT) alloy (a) before wear and (b) 116N.

B. Examination by SEM

SEM observations indicated that all of the worn surfaces of the Al-Si-X alloys had similar appearances when they were worn under similar loads.

At low loads, worn surfaces of the alloys exhibited many parallel tracks or grooves, across which were numerous cavities (Fig. 6.19).

As the load increased, the worn surfaces exhibited fewer cavities and greater plastic deformation. For instance, Fig. 6.20 presents the worn surface of Al-25SiCuMg (PT) alloy after it was worn at 87N. On the worn surfaces, many white strips were observed in the direction of slip. EDS examination indicated that more iron and fewer oxygen were present in the white strip areas (Fig. 6.20 c) than in the other, black areas (Fig. 6.20 d).

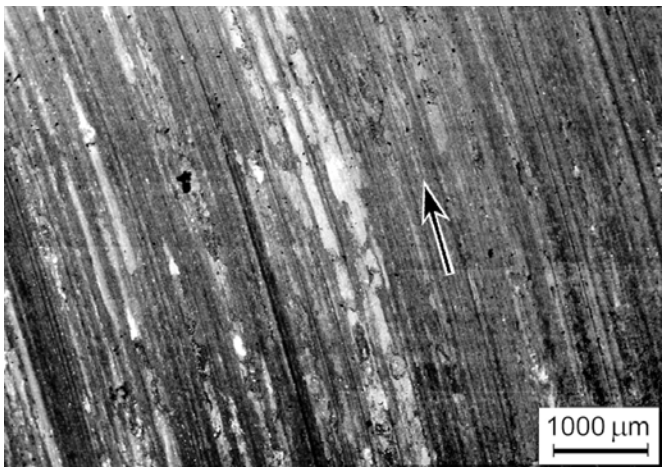

(a)

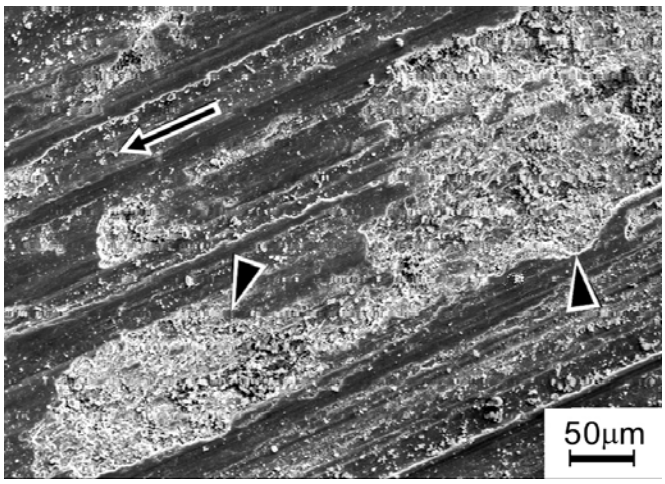

(b)

Figure 6.19 A typical worn surface of Al-Si-X pin after sliding at low loads (a) BEI micrograph of a worn surface tested at a load of 27N for the Al-25SiCuMg (PT) alloy; white strips are verified to be Fe-rich areas. (b) SEI micrograph magnified from the worn surface shown in (a). Triangle arrows indicates the cavities across the sliding tracks, long arrows indicates the sliding direction. [BEI: back-scattered electron image; SEI: secondary electron image]

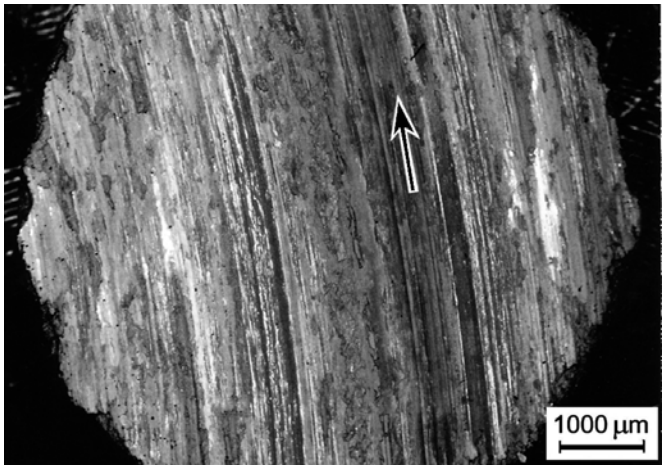

(a)

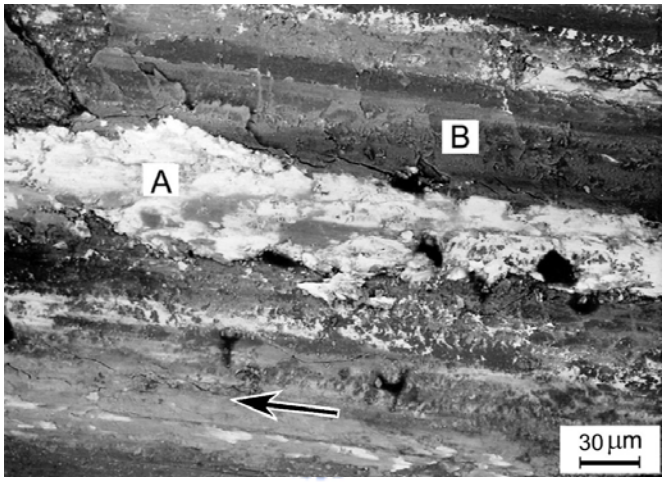

(b)

Figure 6.20 (continued)

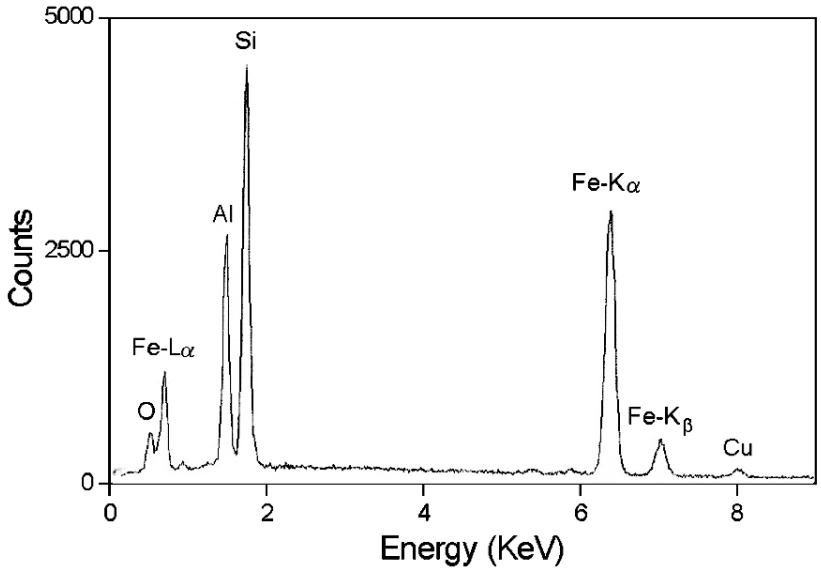

(c)

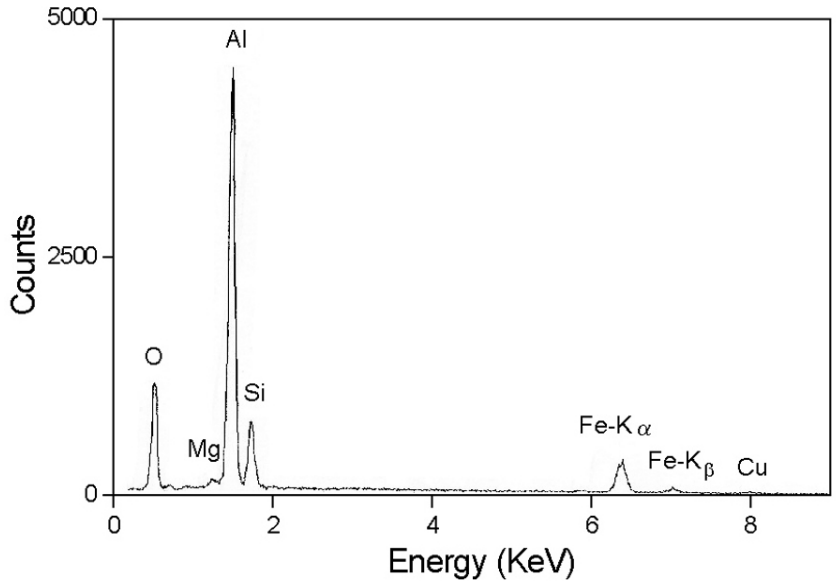

(d)

Figure 6.20 A typical worn surface of Al-Si-X pin after sliding at high loads (a) BEI micrograph of a worn surface obtained on the Al-25SiCuMg (PT) alloy tested at a load of 87N. (b) BEI micrograph showing the magnified image of the worn surface. (c) and (d) are EDS spectra obtained from the area A and area B, respectively. [BEI: back-scattered electron image; EDS: energy dispersive spectrum]

Figure 6.21 shows a typical SEM micrograph perpendicular to the Al-25SiCuMg (PT) surface worn at 87N, which may represent a cross section view of a powder thixocast Al-Si-X surfaces worn at high loads against a steel counterface. A mechanical mixing layer (MML) [19-21] was clearly found to cover the worn surface to a depth of 10 to 50μm. The MML comprised iron and oxygen, as revealed by the EDS analysis shown in Fig. 6.21 b.

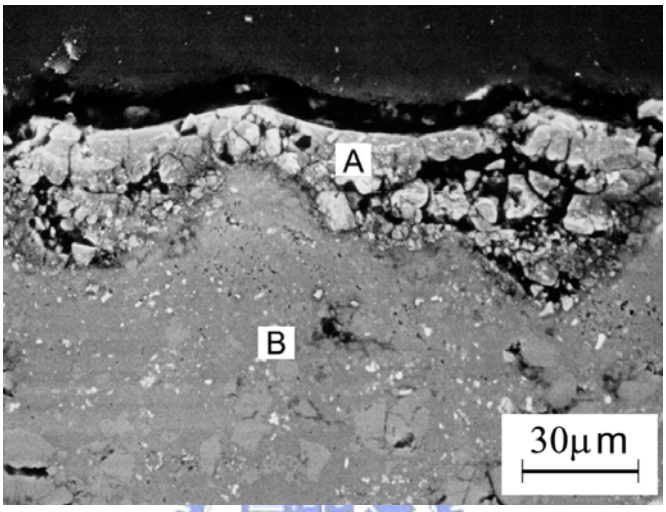

(a)

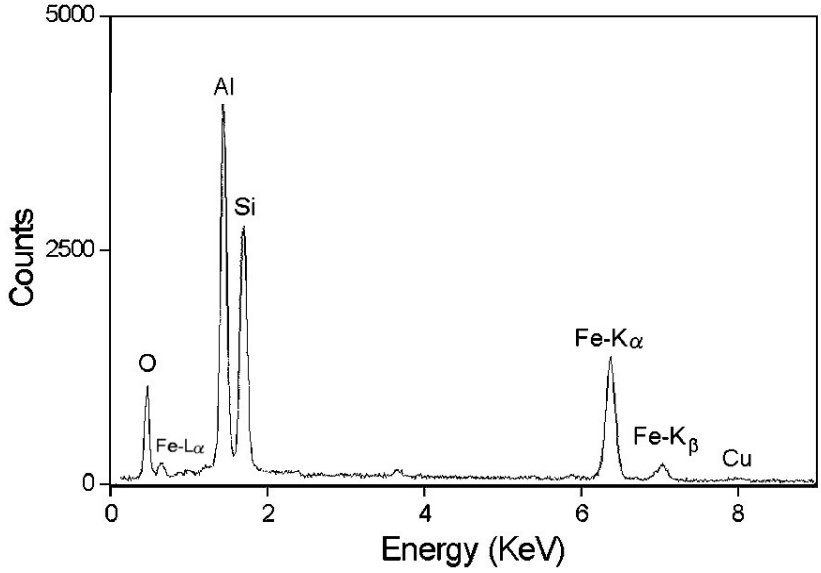

(b)

Figure 6.21 (Continued)

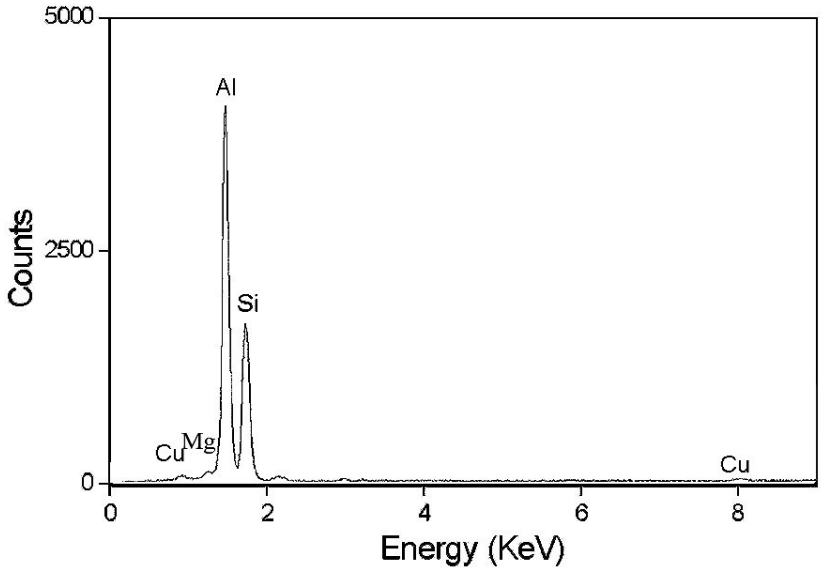

(c)

Figure 6.21 A cross-section of a Al-SiCuMg(PT) surface worn at high loads (a) BEI micrograph of a cross-section perpendicular to the worn surfaces for the Al-25SiCuMg (PT) alloy tested at 87N. The sliding direction is perpendicular to the paper. (b) and (c) are EDS spectra obtained from the area A and area B, respectively. [BEI: back-scattered electron image; EDS: energy dispersive spectrum]

B. Examination by OM

Figure 6.22 presents the typical cross-section optical micrographs of the subsurface for the worn Al-Si-Cu-Mg alloys after seizure. Figure 6.22 a demonstrates that Al-25SiCuMg (PT) had numerous small particles dispersed in the matrix near the worn surface. The dispersed particles were finer as they were nearer the worn surface. The small dispersed particles contained the Si particles and the intermetallic compounds that were fragmented during sliding. A few small cracks are observed near the worn surface of the Al-25SiCuMg (PT) alloy (Fig. 6.22 a). However, many large cracks initiated from the fracture of the primary Si particles were found near the worn surface of the Al-25SiCuMg (IT) alloy (Fig. 6.22 b). The α-Al grains in Fig. 6.22 b were elongated in the direction of sliding, suggesting extensive plastic deformation under the surface of Al-25SiCuMg (IT). LM13 alloy also underwent an extensive deformation near the worn surface (Fig. 6.22 c). The maximum depth of deformation below the worn surface in the present cross-sectional micrographs is 20 to 100 μm.

Figures 6.23 a and b show the optical microstructures of subsurfaces worn at 12N and 87N, respectively. The subsurface worn at 12N showed no plastic deformation; several primary Si particles were found to protrude from the worn surfaces (Fig. 6.23 a), suggesting that the primary Si particles may act as asperities and carry the load during sliding. The MMLs formed on the surface at high load were found to include various fragmented Si particles (Fig. 6.23 b).

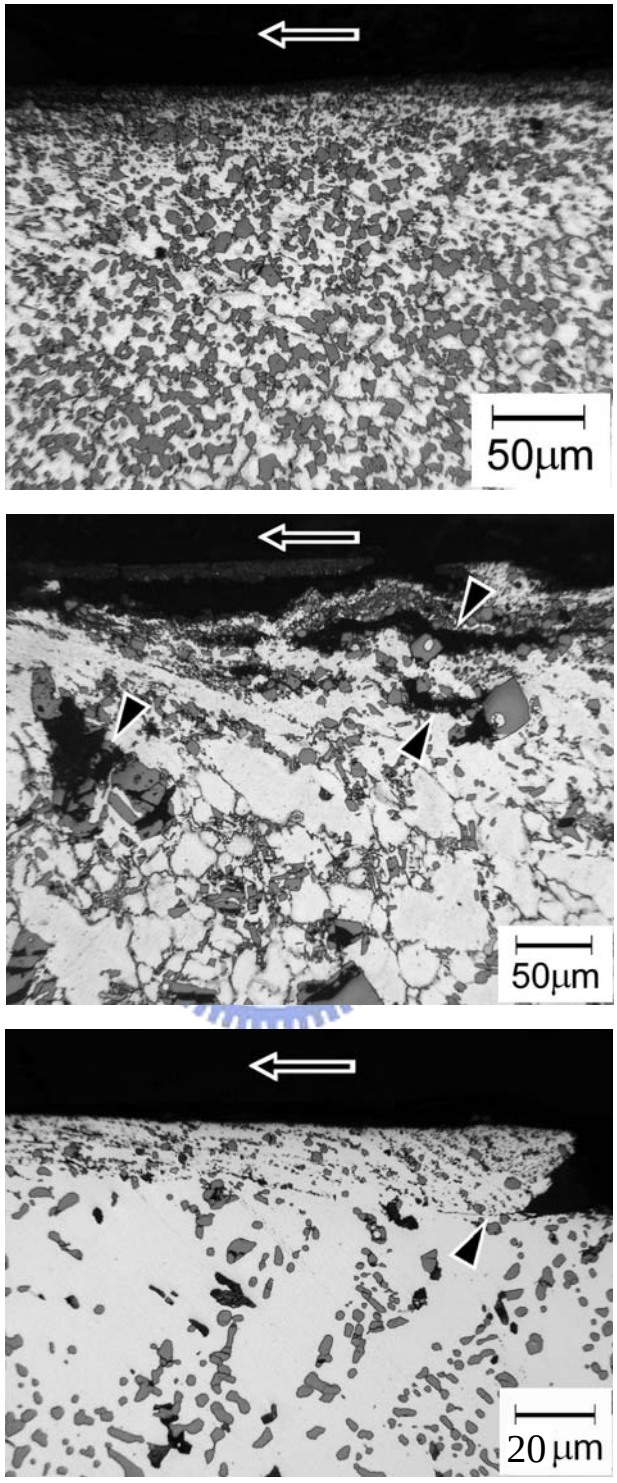

Figure 6.22 OM micrographs of the cross-sections of the worn surfaces , which are observed after seizure and parallel to the sliding direction for (a) as prepared Al-25SiCuMg (PT), (b) as prepared Al-25SiCuMg (IT), and (c) T6-treated LM13 alloys. The upper arrows indicate the sliding direction, and the triangle arrows indicate the cracks in the subsurfaces.

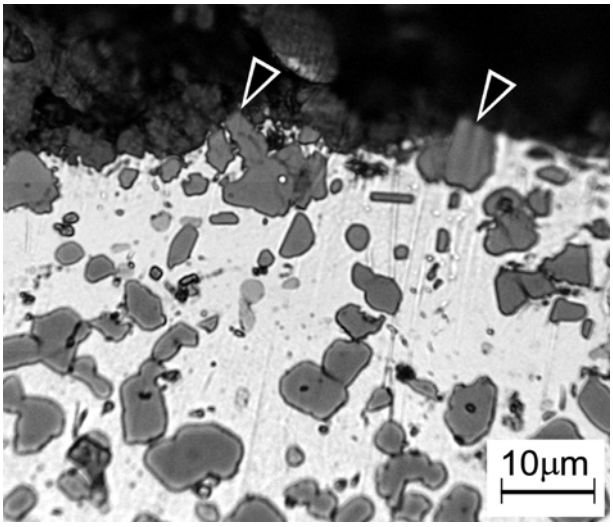

(a)

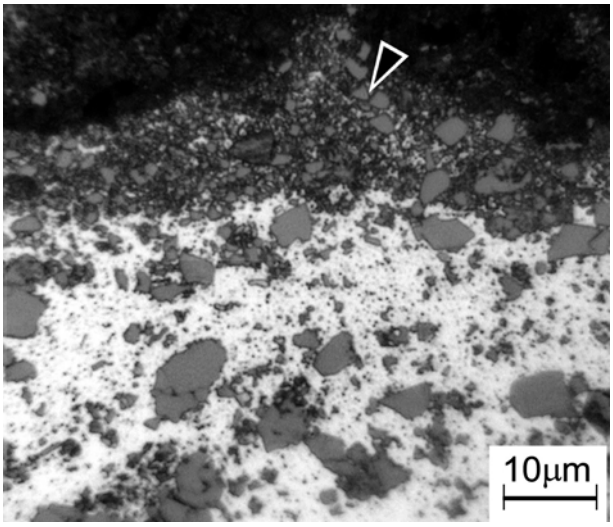

(b)

Figure 6.23 OM micrographs of the cross-sections of the worn surfaces ,which were obtained from as prepared Al-25SiCuMg (PT) alloy after sliding at (a) 12N (b) 87N. The sliding direction is perpendicular to the paper. Arrows indicate the asperities protruding from the sliding surfaces.

6.4.2 Wear debris from the Al-Si-X/ steel sliding wear system

All the Al-Si alloys tested herein were found to yield similar wear debris. Figure 6.24 depicts the wear debris obtained from the sliding of Al-25SiCuMg (PT) at 87 N. The wear debris consists of three types of particles - plate-like flakes, equiaxed particles and long flakes. The long flakes are believed to be the debris delaminated from the iron-rich strip whose area is shown in Fig. 6.20 b, since these strip areas were also found to yield similar EDS spectra that is displayed in Fig. 6.20 c. The size of the equiaxed particles ranges from submicron to several tens of microns (Fig. 6.24b). It is also found that the amount and size of the long iron-rich flakes and plate-like flakes increased with the sliding load.

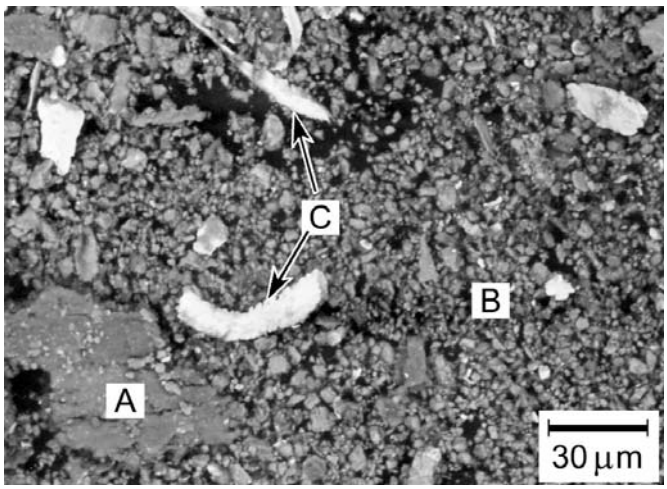

(a)

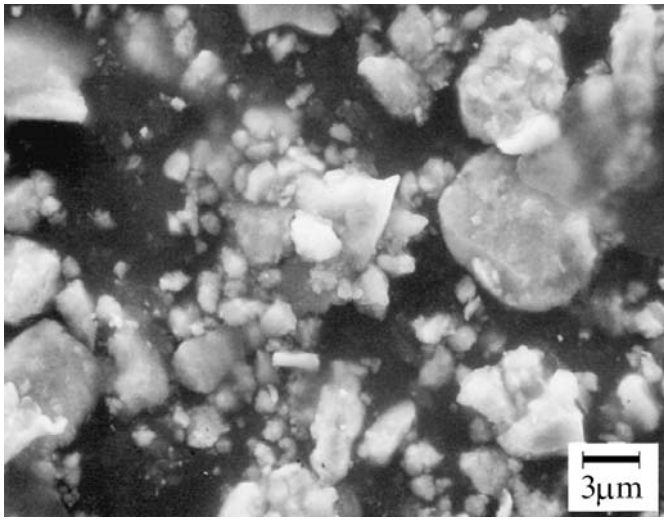

(b)

Figure 6.24 A typical SEM micrographs of wear debris from Al-25SiCuMg (PT)/steel wearing system

The wear debris obtained at a load of 87N. (a) A typical BEI micrograph, showing a mixture of A- plate-like flakes, B- fine equiaxed particles, and C- long iron-rich flakes. (b) A magnified secondary electrons image (SEI) of the fine equiaxed particles.

6.3.3 Bulk surface sliding temperature

The surface temperatures were measured using a thermal couple in contact with the worn surface immediately after stop sliding of each 20-minute sliding tests. These measured temperatures are regarded as the bulk surface temperatures in the steady state.

Figure 6.25 presents the measured surface temperature of the as-prepared Al-Si-Cu-Mg alloys. At low loads, below about 70N, LM13 alloy was found to have the highest measured temperature, and Al-25SiCuMg (IT) alloy to have the lowest. However, as the load further increased, the temperature of Al-25SiCuMg (PT) alloy slowly came to exceed that of the other two alloys (Fig. 6.25).

T6-treated Al-Si-Cu-Mg alloys exhibited similar trends in temperature, but the values were slightly smaller than those of the as-prepared alloys shown in Fig.6.25.

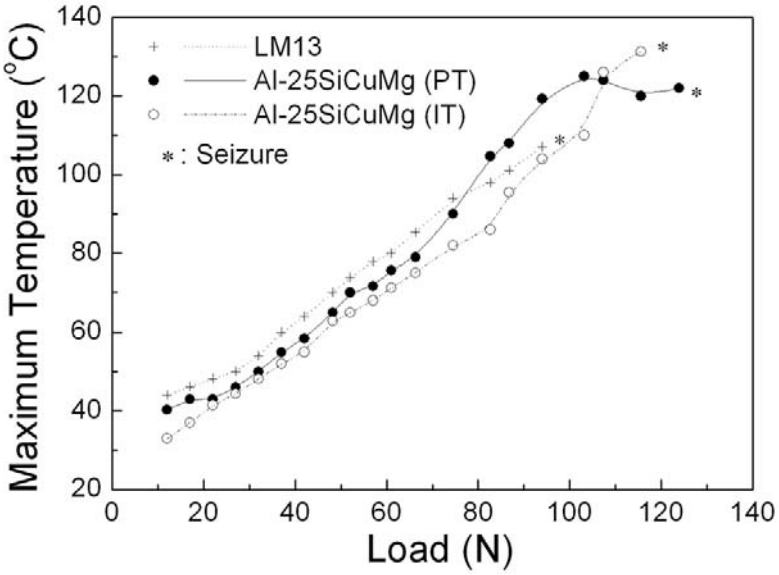

Figure 6.25 Variation with load of sliding surface temperature for the as prepared Al-Si-Cu-Mg alloys.

6.5 Discussions

6.5.1 Wear behaviors at low loading conditions (region I)

A. Wear rates

Wear rates of the four Al-Si-X alloys tested under low load (region I) were found strongly depended on their hardness and primary Si particle size.

The wear rates of the Al-Si-X alloys at low loads increased linearly with the load (Fig. 6.12). The linearity can be explained using the Archard model [115]. This model is detailed in Section 6.2.3 in this Chapter. When wear is tested at low loads, plastic deformation is localized at the real contact spots or asperities on the sliding surfaces. In the Archard model, the wear loss is hypothesized to be related to the volume of the debris detached from the real contact asperities that have been plastically deformed and adhere to a counter surface. Based on this assumption, the volume of wear (W) after sliding through a distance (d) is given by W/d=(KL)/(3H), where K is a wear rate constant; L is the nominal applied force, and H is the penetration hardness of the surface material that is being worn away.

Harder materials are expected to have greater wear resistance, according to Archard model. The Al-25SiCuMg (PT) alloy in T6 condition has the highest hardness of all the tested alloys (Table 2). This fact explains why the T6-treated Al-25SiCuMg (PT) alloy had a much lower wear rate than the others at low loads (Fig. 6.12 b).

Archard's equation predicts that the wear rate of a material is mainly depended on its hardness. However, an exception of this proportional relationship between hardness and wear resistance was found in this study. Al-25SiCuMg (IT) alloy had a lower wear resistance than LM13 in T6 condition (Fig. 6.12b), although the hardness exceeded that of the latter (152Hv against 141Hv). This exception is associated with the large primary Si particles in Al-25SiCuMg (IT). The problem of the effect of large primary Si particles on the wear performance of hypereutectic alloys has been discussed [49], discussed in the following paragraph.

High wear resistance of hypereutectic Al-Si alloys is known to be mostly attributed to the presence of hard primary Si particles. Therefore, higher Si content is expected to

decrease wear rate. In this study Al-25SiCuMg (IT) has 25%Si, much larger than that of 12% in LM13; however, the alloy in T6 state performed worse in wear than LM13 (region I in Fig. 6.12b). On the other hand, Al-25SiCuMg (PT) also has similar content with Al-25SiCuMg (IT), but it showed much higher wear resistance than LM13 alloy. The difference in wear behavior of the two alloys is attributed to their distinct Si particle morphologies. The large Si particles in Al-25SiCuMg (IT) tend to be fractured (Fig. 6.22b) and worn off during sliding, increasing the wear rate of the alloy. Therefore, the distribution and size of the primary silicon particles, rather than the overall silicon content of the alloy, should be more important in wear performance in this case.

From the above discussions, the superior performance of the T6-treated Al-25SiCuMg (PT) follows from not only the high microhardness of the alloy, but also the unique characteristics of fine and uniform Si particles fabricated by powder thixocasting process in this work.

B. Coefficient of frictions

The coefficients of friction measured in the Al-Si-X/steel system sliding under low load (region I) are suggested to be greatly affected by the size and distribution of the primary Si particles.

Figure 6.26 schematically depict the cross-sections of the three Al-Si-Cu-Mg alloys during sliding, to elucidate the mechanisms for the frictional traction. These diagrams were based on the microstructural observations of the worn subsurfaces. The model in Fig. 6.26 may explain why the coefficients of friction follow the order, LM13 >Al-25SiCuMg (PT)> Al-25SiCuMg (IT), under the same wearing conditions, at low loads (region I in Fig. 6.14).

In Fig. 6.26, the materials just below the worn surface showed no plastic deformation at low loads. As sliding proceeded, some of the primary Si particles protruded from the worn surfaces (Fig. 6.23a). During the initial stage of sliding, the hard Si protuberances may plough the steel counter surface, causing material to be transferred from the steel surface, so separated thin iron-rich strips were formed on the aluminum worn surfaces (Fig. 6.19 a).

The actual contacts between the sliding surfaces are well known to be localized only at some individual spots, called asperities, on a microscopic scale. The higher affinity of the asperities to adhere to the steel counter surfaces results in the larger frictional traction during sliding. Figure 6.26 depicts the primary Si particles protrude from the worn surfaces during slide wearing. These protrusions may act as points of contact with the steel counter body to carry most of the sliding load. The larger Si particles are responsible for the generation of the larger protuberances on the worn surfaces, reducing the opportunity for the α-Al matrix to come into contact with the steel counterbody, reducing the frictional traction.

Greater contact of aluminum asperities is responsible for higher frictional traction, because aluminum is prone to adhere to a steel surface. However, stronger contact of Si particles corresponds to lower frictional traction, because Si particles cannot easily adhere to the steel counterface and they may become fractured and thus acts as a solid lubricant. Hence, the larger primary Si particle or a higher Si content is postulated to reduce the frictional traction. This assertion is consistent with the fact that the LM13 (~12%Si) alloy has a higher frictional traction at low load than the Al-25SiCuMg alloys (~25%Si). And, the coefficient of frictional for Al-25SiCuMg (IT) alloy is lower than that for Al-25SiCuMg (PT) alloy in region I of Fig. 6.14.

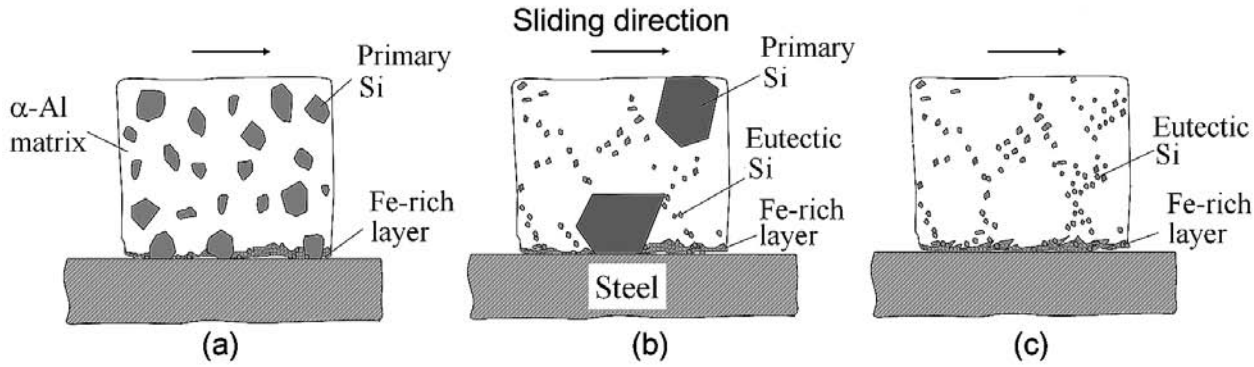

Figure 6.26 Schematic diagrams of the cross sections perpendicular to the sliding surfaces at low loads.

(a) Al-25SiCuMg (PT), (b) Al-25SiCuMg (IT) and (c) LM13 alloys.

6.5.2 Wear behaviors at high loading conditions (regions II/III)

A. Wear rates in region II do not simply related to high temperature compressive strength

There are no strong relationship between high temperature compressive strength and wear resistance for the investigated Al-Si-X alloys, despite that sliding under heavy load inevitably result in high temperature at the sliding surface [120,121]. For example, even though the Al-20SiFe (PT) alloy possesses lower compressive strength than conventional alloys (Fig. 5.9), it still has higher resistance in wear in region II than conventional alloys (Fig. 6.12 a) This suggests that the wear mechanism of region II should not be simply attributed to compressive strength or flow strength of the materials at elevated temperature in this case.

B. Mechanical mixing layers (MMLs)

In this study, mechanical mixing layers (MMLs) were typically found to form on the sliding surfaces of Al-Si-X alloys when they slid against a steel counter body. It is believed the MMLs greatly affect the wear behaviors of these alloys sliding at high loads (in regions II/III).

The MML is generated by the mutual transfer of materials between the two contact surfaces and is normally accompanied by an extensive surface deformation [122-129]. The compositions and microstructures in the MML also vary with the sliding load. In a Al-Si/steel sliding system, at low load the MML consists of a matrix of ultrafine α-Al grains dispersed with small α-Fe particles, and no intermetallic compound or oxides are generated at low load [126-128]; whereas, at high loads the MML consists of nanosized particles of Fe-Al(Si) intermetallic compounds, aluminum and iron oxides that are dispersed in the ultrafine α-Al matrix. The MML contains these ultra-fine microstructures, and so can effectively protect the surface from wear [128].

These microstructural characteristics of the MML described in [126-128] match those identified herein. At low loads, several Fe-rich strips were present on the sliding surfaces (Fig. 6.19 a). These Fe-rich strips can be regarded as a species of MML that is

formed at low load. However, the Fe-rich strips formed at low loads should be very thin, since there was little subsurface deformation occurred in low load sliding conditions. As the sliding load was increased, a significant quantity of aluminum oxide was detected on the worn surface (Fig. 6.17 c). The formation of oxide is consistent with that in [120], which states that the sliding surface of Al-Si alloys may be oxidized by the oxidizing atmosphere and the increase in the high surface temperature by the heavy sliding load. The MML formed at high load was found to include Fe element (Fig. 6.21 b), and many fine Si particles embedded in a severely deformed Al matrix (Fig. 6.23 b). The MML formed at high load was also determined herein to exhibit very high hardness, of up to approximately 600Hv.

Figure 6.27 depicts a schematic diagram to elucidate the wear behaviors of the Al-25SiCuMg (PT) alloy at high load. This proposed figure is based on the microstructural observations of the worn surfaces and subsurfaces.

In Fig. 6.27, a plastic deformation zone below the worn surface is exhibited. In this deformation zone, many cracks are initiated from the sites of the fractured Si particles, suggesting that large flakes of debris may be detached from these cracks. A mechanical mixing layer (MML) is present on the worn surface of the alloy. Some cracks are present in the MML, which is deduced from the fact that long Fe-rich flakes were present in the debris (Fig. 6.24 a); and, these flakes are posited to be delaminated from the cracks in the MMLs.

Figure 6.27 also schematically show that the subsurface region of a worn Al-25SiCuMg (PT) alloy contains fragmented Si particles (Fig. 6.23 b). The fragmentation of Si particles in Al-Si alloys by plastic deformation was proposed by Pramila [122], and is schematically shown in Fig. 6.28. It shows that the fragmentation is a function of stain that the matrix experience.

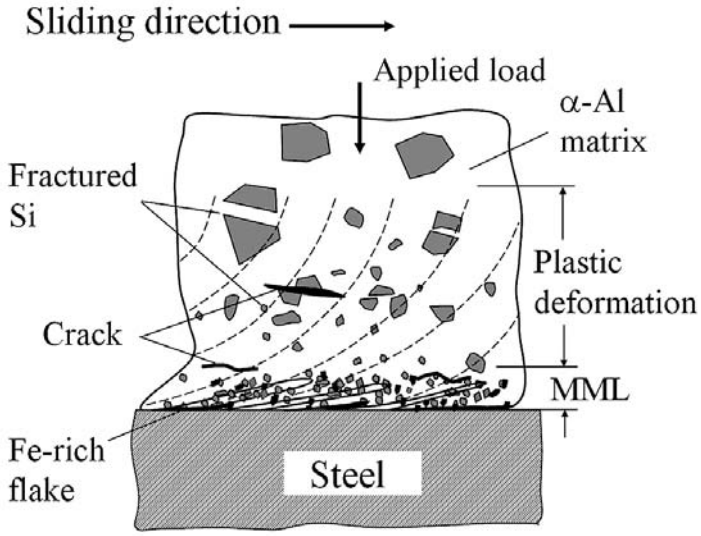

Figure 6.27 Schematic diagrams of the cross section perpendicular to the surface sliding under heavy load for the hypereutectic Al-Si alloys.

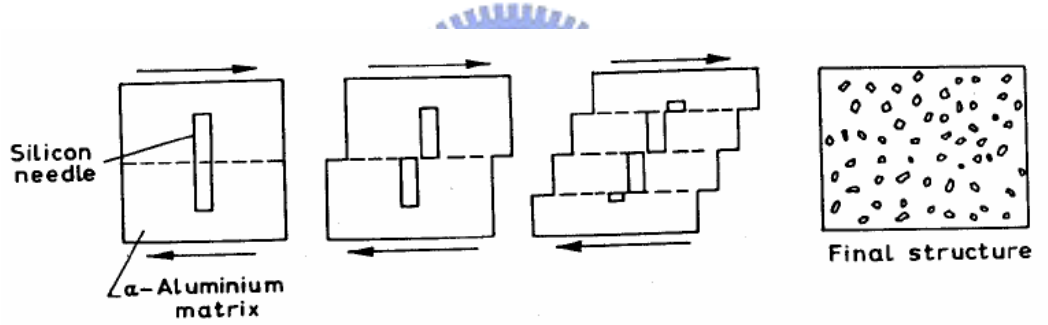

Figure 6.28 Fragmentation process of Si particles by shearing deformation [122]

C. Transition from region I to region (II/III)- subsurface deformation

A transition of the wear rate from region I to region II is evident for the as-thixocast Al-25SiCuMg (PT) and Al-20SiFe (PT) alloys and T6-treated Al-25SiCuMg (PT) alloy (Fig. 6.12). The transition is important for the powder thixocast alloy because it clearly dramatically improve the wear performance of this alloy under high-load sliding conditions.

As is mentioned in above, the formation of MMLs can effectively protect the surfaces from wear. However, the wear rate of Al-25SiCuMg (PT) continuously

increased with the load below 67N (region I in Fig. 6.12), in spite of the production of the MMLs. In contrast, the wear rate began to drop as the load increased to 67N (Fig. 6.12). The MMLs were generated under a wide range of loads for Al-Si/steel sliding systems [124-126], but the transition is related only to a critical load. This difference reveals that the MMLs formed at high loads (in region II) seem to be much “stronger” than those formed at low loads (in region I).

The fact that the “stronger” MMLs are formed at high loads is attributable to the plastic deformation and the oxidation on the surface or subsurface material. Two factors can mainly affect the strength of the Al-Si surface during sliding wear - the rise in surface temperature and the intention of subsurface plastic deformation. A high surface temperature usually softens the sliding surface material by dynamic recovery or recrystallization or coarsening of age hardened precipitates [26]. However, plastic deformation strengthens the surface material by work hardening, generating microstructures that comprise elongated subgrains or textures [122]. Additionally, a large plastic deformation may also involve ultra fine oxides or intermetallic compound particles dispersed in the subsurface matrix through a process that is similar to mechanical alloying [122,126]. Consequently, the transition observed herein is suggested to be “triggered” by a critical intense subsurface deformation, as it was accompanied by the “stronger” MMLs.

The coefficient of friction on the Al-25SiCuMg (PT) alloy became rising and unstable when the load increased to the transition point, 67N (Fig. 6.13 a). This rising in the coefficient of friction at the transition can be explained using the aforementioned suggestion that an extensive subsurface deformation should be responsible for the transition. In beginning of the wearing test, the large Si particles that protrude from the surfaces served as points of contact during sliding at low loads (Fig. 6.26). These protruding Si particles prevented the α-aluminum matrix from touching and adhering to the steel counter surfaces. Accordingly, the Al-25SiCuMg (PT) alloy had a low coefficient of friction at low load (region I in Fig.6.13 a), since the Si particles have a low affinity to the counter surface. However, as the sliding proceeded, the temperature of the sliding surface increased continuously with the sliding load (Fig. 6.25), gradually softening the α-aluminum matrix. When the external stress yielded by the

frictional traction and the applied load exceeded the flow strength of the aluminum matrix, the aluminum matrix would begin to be plastically deformed. Consequently, the plastic flow of the matrix fractured the primary Si particles (Fig. 6.27). As the large primary Si particles were broken down into small particles, the aluminum matrix came into contact with, and adhered to, the steel counter surface, increasing the coefficient of friction (region II in Fig. 6.13 a) because of the high affinity of aluminum to the steel surface.

However, the coefficient of friction of LM13 was found to drop as the load increased to the transition load of above 67N (Fig. 6.13 b). The behavior of the LM13 alloy is exactly opposite that of the Al-25SiCuMg (PT) alloy (Figs. 6.13 a and b). This drop in the coefficient of friction is regarded as similar to the behavior of region III for the powder thixocast alloy presented in Fig. 6.13 a, because the as-prepared LM13 alloy did not give any drop in wear rate at high loads, as displayed by the powder thixocast alloy in the region II (Fig. 6.12 a). The drop in the coefficient of friction in region III for the Al-Si alloys is attributable to the softening of the material at its sliding surface and the high wear rate during sliding at high loads. Figure 15 demonstrates that LM13 has lower compressive strength than Al-25SiCuMg (PT) alloy, revealing that LM13 alloy could have more intense plastic deformation than that did Al-25SiCuMg (PT) alloy during heavy load sliding. However, the large deformation of LM13 at high loads also accelerates the formation of wear debris by delamination [27] Moreover, the large amount of wear debris may act as a solid lubricant, reducing the ability of the “fresh” aluminum matrix to adhere to the steel counterbody and thereby reducing the frictional traction in region III (Fig. 6.13 b). In contrast, the Al-25SiCuMg (PT) alloy was found to have a very low wear rate in region II (Fig. 6.12), suggesting that the protective MMLs formed on the sliding surface were more stable for Al-25SiCuMg (PT) than for LM13. Hence, the reduction by the debris lubricant of the coefficient of friction for the Al-25SiCuMg (PT) alloy is weak, leading to the different behaviors in the coefficient of friction between Al-25SiCuMg (PT) and LM13 when the sliding load was increased just above 67N (Fig. 6.13 a and b).

From the above discussions, it is therefore concluded that the superior wear performance for Al-25SiCuMg (PT) alloy is not only because of its high hardness but

also because of its fine primary Si particles through the unique process of powder thixocast, since the fine Si particles can effectively suppress the delaminating rate of MMLs.

6.5.3 Estimation of the flash sliding-surface-temperature

Flash surface temperature during sliding was estimated by the compressive strength (Fig. 5.9) and the bulk surface temperature (Fig. 6.25); besides, the mechanism of subsurface deformation that is mentioned in Section 4.2.2., to be responsible for the transition of wear to region II, is also discussed in the followings.

The real contact between two sliding surfaces is limited only on the protrusive asperities. The external force exerted on the sliding surface includes the normal applied load L, and the frictional traction F. The protrusive asperities are deformed to carry the external imposed force (L+F), so the real contact area A_r equals $(L+F)/\rho_f$, where ρ_f refers to the flow stress of the deformed asperities. F is normally about 0.5L; besides, F and L are assumed to be additive for simplicity. Then, the real contact area A_r is around $1.5L/\rho_f$. Hence, A_r will increase with the applied load L. The transition probably occurred when A_r rose to near the nominal sliding area A_n, resulting in the extensive subsurface deformation. This hypothesis is identical to that proposed to explain the mechanism of wear seizure [118,119]. However, the seizure may not occur under this condition for the hypereutectic and eutectic Al-Si-Cu-Mg alloys, because plenty Si particles may act as an anti-seizure agent to increase the seizure strength of the alloys [130].

Based on the aforementioned hypothesis, the transition occurs only if the nominal applied pressure (L/A_n) is increased to approximately $\rho_f/1.5$, because the criterion for transition is $A_r = A_n = 1.5L/\rho_f$. At the transition, the nominal applied pressure was about 1.25MPa (67N) (Fig. 6.12) and the surface temperature at this load was about 80 °C (Fig.6.25). However, the compressive strength (referred to as ρ_f) of the Al-25SiCuMg (PT) alloy at 80 °C is about 400MPa (Fig. 6.9), indicating that the applied external pressure of 1.25MPa is not likely to cause the subsurface deformation, as the surface material still has a very high flow strength of 400MPa. Hence, the aforementioned criterion $A_r = A_n$ assumed to apply to the transition, seems

unreasonable. This puzzle is because that there is flash surface temperature that is far larger than the measured surface temperature, and in reality A_r is not likely increase to A_n.

The real points of contact always undergo a large deformation and most of the work done in plastic deformation is transformed into heat. Accordingly, the contact spot will have a localized temperature, called flash surface temperature (T_f), which exceeds the average surface temperature, called bulk surface temperature (T_b) [119]. However, these real localized points of contact are very small, and they may move during sliding. Therefore, the flash temperature is very difficult to measure accurately, and has seldom been reported. Many researchers proposed various models to predict the flash temperature [119]. Spurr [121] developed an acceptable following relationship between T_f and T_b; $T_f = T_b + K\mu L^{1/2} H^{1/2} \upsilon$, where μ is the coefficient of friction; L is the applied load; H is the hardness of the specimen; υ is the sliding speed, and K is a constant that specifies a shape factor and is related to the thermal characteristics of the pin and disc. However, all these predicted values were sensitive to the coverage rate of surface oxides and the number of the contact asperities, so they were varied over a wide range from several tens to hundreds of degrees [120].

In reality, surface roughness or vibration during sliding may cause the load distribution to fluctuate. Furthermore, if the sliding surfaces have hard protuberances, such as primary Si particles, then these protuberances may suffer a localized impact force during sliding, leading to unevenly or instant forces to the surfaces. Therefore, in reality, it is hardly to have the two sliding surfaces to completely mutually contact, so A_r is not likely to be equal to A_n even when sliding occurs under heavy loads. Consequently, the criterion that applied to the transition my be $A_r = kA_n$, where k is a number between zero and one. The value of k may be associated with the possibility to completely mutually contact in the sliding system. If the external force or the surface temperature was distributed more uniformly throughout the contact surface and the surface roughness was smaller, the value of k could be more close to unity.

The flash surface temperature (T_f) at the transition may be approximately estimated from the presented results and the proposed criterion for the transition. At

the transition, the flow strength ρ_f of the sliding surface material is therefore approximately 1.5P/k, since $A_r = kA_n = 1.5L/\rho_f$, and $P=L/A_n$, where P is the nominal applied pressure at the transition, 1.25MPa (67N) (Fig. 6.12). Although the exact value of k remains unknown, the value of k is probably not very low, since at the transition, the subsurface was greatly deformed. If k=0.01 to 0.1 is assumed, the estimated flow strength ρ_f should be 18.75 to 187.5 MPa. If the flow strength was equal to the compressive strength of the alloy (Fig. 6.9), then the flash surface temperature must be 350°C to 500°C. However, the bulk surface temperature was measured to be about only 80°C at the transition (67N in Fig. 6.25), indicating that the flash temperature during sliding must be much higher than the bulk temperature. This assertion also agrees with the intense surface oxidation found in this work (Fig. 6.17 c), as the flash temperature increased drastically because the surface oxides could suppress the dissipation of frictional heat [120].

6.5.4 A proposed mechanism for wear behaviors of the Al-Si-Cu-Mg Alloys

From the aforementioned discussions, it is known that wear resistance of Al-Si alloys is a function of not only Si content or distribution and sizes of primary Si particles but also the heat treatment state and alloying element additions. Two wearing mechanisms, asperity adhesion and plastic delamination, will be applied to make a brief summery of the wear results obtained in this study.

The plot of wear rate as a function of load was found to be clearly divided into the three regions-I, II, and III for the powder thixocast Al-Si alloy (Figs. 6.12). However, the similar regions were not clearly found for the conventional Al-Si alloys. Figure 6.29 schematically shows a plot of wear rates to explain the wear behaviors.

The wear rates of the alloys are suggested in Fig. 6.29 to involve the two mechanisms - asperity adhesion and plastic delamination. The two mechanisms consist with the observations of the wear debris. The wear debris formed at various loads was found to always comprise the two different types - equiaxed particles and plate-like or strip-like flakes (Fig. 6.24). Besides, the flakes apparently formed increasingly with load during wear at high loads; whereas, the equiaxed particles did not. The flakes of the debris were considered associated with the wear mechanism of plastic delamination;

whereas, the equiaxed particles were with the mechanism of asperity adhesion. The wear rate is a summation of the formation rates of the two types of debris. Therefore, it includes the two portions associated with the mechanisms - asperity adhesion and plastic delamination respectively, as shown in Fig. 6.29.

At low sliding loads, the wear debris was found to mostly comprise the small equiaxed particles. These equiaxed particles were formed due to the fracture of the contact asperities during wear, since the surface deformation is constrained mostly on the asperities, as shown in the inset of Fig. 6.29 at low loads. Nevertheless, the wear debris formed at low loads was also found to include some flakes. These flakes were believed to be delaminated from the worn surface and thus caused the worn surface to be pitted as shown in Fig. 6.19b. However, the amount of these flakes was found to be far less than that of the equiaxed particles at low loads. These delamination rates of the flaks are shown in Fig. 6.29 to be the curves B and B' for the powder thixocast alloy and the conventional alloy, respectively.

As the sliding load increased, the subsurface deformation increased significantly. Thus, the surface material was hardened by the plastic deformation through the effects such as strain hardening and formation of MMLs. This increase in hardness of the surface material leaded to a low formation rate of the equiaxed particles, and thus leaded to a transition in the plot of the wear rate associated with the asperity adhesion, i.e. the cure A shown in Fig. 6.29. However, as load further increased, the formation rate of the flakes also increased due to the delaminating of MMLs by the intensive subsurface deformation. Since the MMLs protected the sliding surface from wear at high loads, the wear rate should be mostly depended on the rates of formation and delamination of the MMLs at high sliding loads. If the MMLs formed continuously and they were not delaminated at all, the wear rates of these alloys should decrease with load. Besides, it may be reasonable to consider that the three Al-Si alloys have similar formation rates of the MMLs, since they have similar constituents. Thus, the wear rate associated with mechanism of asperity adhesion should decrease with load after the transition, as shown in Fig. 6.29 to be the curve A. Based on the above discussions, the wear rates at high loads should be dominated by the delamination rates of the MMLs for these alloys. The delamination rate of MMLs should increase more quickly with load for the conventional

alloys than for the powder thixocast alloy (curve B' against B in Fig. 6.29). This hypothesis consists with the facts that the subsurface cracks were found initiated from the fracture sites of large Si particles (Fig. 6.22 b) or in the softer matrix (Fig. 6.22c). When the load further increased, the delamination rate of the MMLs could be larger than the formation rate of the MMLs, so that the wear rate would increase again due to a severe wear from the subsurface under the MMLs. From the above discussions, it is therefore concluded that the superior wear performance observed for Al-25SiCuMg (PT) alloy is mainly attributed by the refinement of primary Si through the unique process of powder thixocast, since the refinement can suppress effectively the delamination of MMLs.

The wear rate of an Al-Si/steel sliding system normally involves mild and severe wear regions, according to the applied load [23]. At low load, the wear rate increases almost linearly with the load, as in mild wear; at high loads, the wear rate increases very rapidly with load, as in severe wear [23]. The mild wear can be the wear of region I (Fig. 6.12); whereas, the severe wear may correspond to the wear of region III herein (Fig. 6.12). However, region II (Fig. 6.12) observed for the powder thixocast alloy in this study involved a drop in wear rate with load. The drop in wear rate with load is rather unusual and differs from the mild and severe wear. In fact, the region II has seldom been reported for conventional Al-Si alloys [131]. The wear results and mechanisms of the three wear regions I, II and III are discussed as follows.

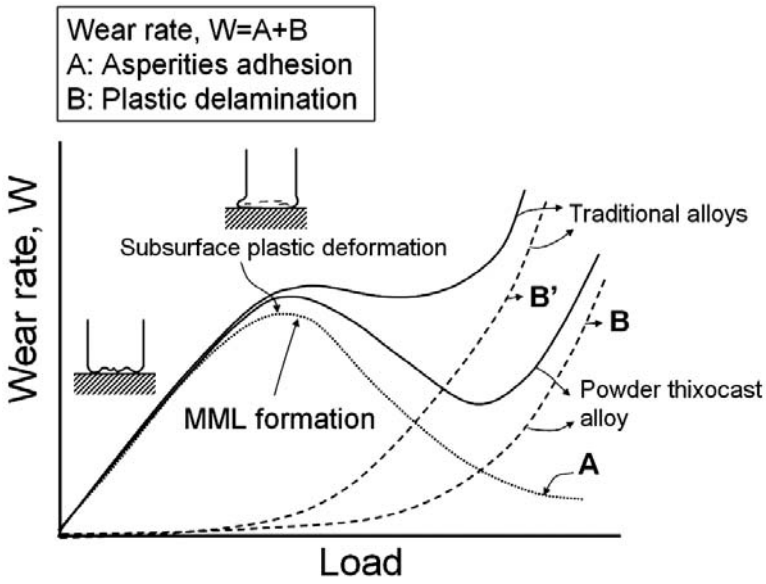

Figure 6.29 Schematic plots of wear rate as a function of sliding load for powder-thixocast and conventional alloys.

It is considered that wear rates, w, are divided into two portions - A: the portion of wear rate caused by asperities adhesion, and B by plastic delamination.

6.6 Conclusions

Dry sliding wear behaviors of two powder-thixocast alloys, Al-25Si-2.5Cu-1Mg (PT) and Al-20Si-5Fe (PT) were investigated. For comparison, two conventional alloys, Al-25Si-2.5Cu-1Mg (IT) and LM13, fabricated by traditional routes were also examined. The following conclusions can be drawn.

1. Al-25Si-2.5Cu-1Mg (PT) alloy showed greater wear resistance than that of the conventional alloys, owing to its finer Si particles and higher hardness. However, Al-20Si-5Fe (PT) powder-thixocast alloy shows lower wear resistance at low loads than that of the conventional alloys despite of its fine microstructure, owing to its low hardness.

2. The plots of the wear rate of the powder thixocast alloy varied with the load could be divided into three regions. The wear rate increased about linearly with the load below 67N (region I); it then slowly decreased as the load increased from 67N to

97N (region II). It finally slowly increased to seizure (region III). The transition from wear region I to region II is attributable to the formation of the mechanical mixed layer (MML) generated by plastic deformation of a heavy loaded worn surface. The transition from wear region II to region III is probably governed by the delamination of MML under more severe load conditions.

3. The MMLs formed at high loads herein contain plenty of hard particles of Si, Fe and Al_2O_3 phases embedded in an α-Al matrix. The formation of the MMLs was accompanied by a large plastic deformation of the material that is adjacent to the sliding surface.

4. The formation of stable mechanical mixing layers (MMLs) on sliding surfaces is responsible for the superior wear performance of the powder thixocast alloy. In contrast, the formation of MMLs was found to have less beneficial effect on the conventional Al-Si-Cu-Mg alloys. This difference is attributable to the fact that the delamination rate of MMLs in the conventional alloys is higher than that in the powder thixocast alloy, because subsurface cracks tend to be generated from the sites of the fractured large Si particles or the soft matrix of the conventional eutectic Al-Si-Cu-Mg alloys.